

## Antimicrobial Modification of PET by Insertion of Menthoxy-Triazine

Jiyu Li,<sup>#</sup> Pengfei Zhang,<sup>#</sup> Mei Yang, Zixu Xie, Guofeng Li,<sup>\*</sup> and Xing Wang<sup>\*</sup>Cite This: <https://doi.org/10.1021/acscapm.1c01775>

Read Online

ACCESS |



Metrics &amp; More



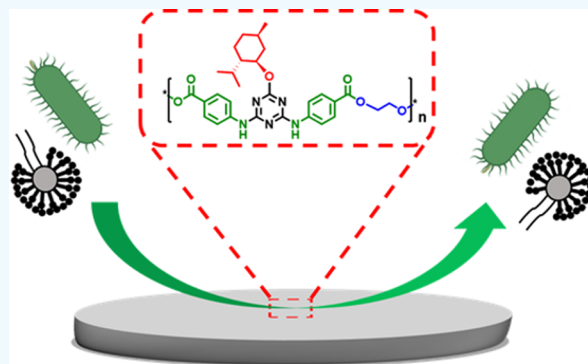
Article Recommendations



Supporting Information

**ABSTRACT:** Microbial contamination on polyethylene terephthalate (PET) negatively affects human health. Thus, there is still a challenge endowing PET with nonleaching antimicrobial performance. Here, menthoxytriazine was inserted into the backbone of PET, named PEMT, through polycondensation between ethylene glycol (EG) with 2-menthol-4,6-aminobenzoic-1,3,5-triazine (DPMT). The antimicrobial adhesion performances of PEMT were evaluated by antibacterial adhesion test and antifungal landing test. The antibacterial adhesion test indicated that the PEMT possessed better antibacterial adhesion capability than raw PET, achieving 93.3% and 88.3% resistance against *Escherichia coli* (Gram-negative) and *Staphylococcus aureus* (Gram-positive). An antifungal landing test exhibited that PEMT had better resistance to *Aspergillus niger* (fungi) contamination compared to PET. Zone of inhibition, water contact angle, and BacLight live/dead fluorescent experiments were used for a deeper analysis, illustrating that the stereochemical structure of menthoxy group played a key role in the antimicrobial adhesion mechanism. In addition, the results of MTT assay illustrated the PEMT was a noncytotoxic material. This work presents an effective strategy for the antimicrobial adhesion modification of PET.

**KEYWORDS:** antimicrobial adhesion, PET, menthol, menthoxy-triazine, stereochemistry



## 1. INTRODUCTION

Polyethylene terephthalate (PET), as a polymer with low cost and excellent performance, has been widely applied in medical textiles and medical devices.<sup>1–3</sup> However, due to poor antimicrobial properties, the surface of PET is susceptible to microbial contamination, which can easily lead to serious nosocomial cross-infection.<sup>4,5</sup> With the increasing demand of human healthcare, the antimicrobial modification of PET has become a popular research topic in the field of polymers.

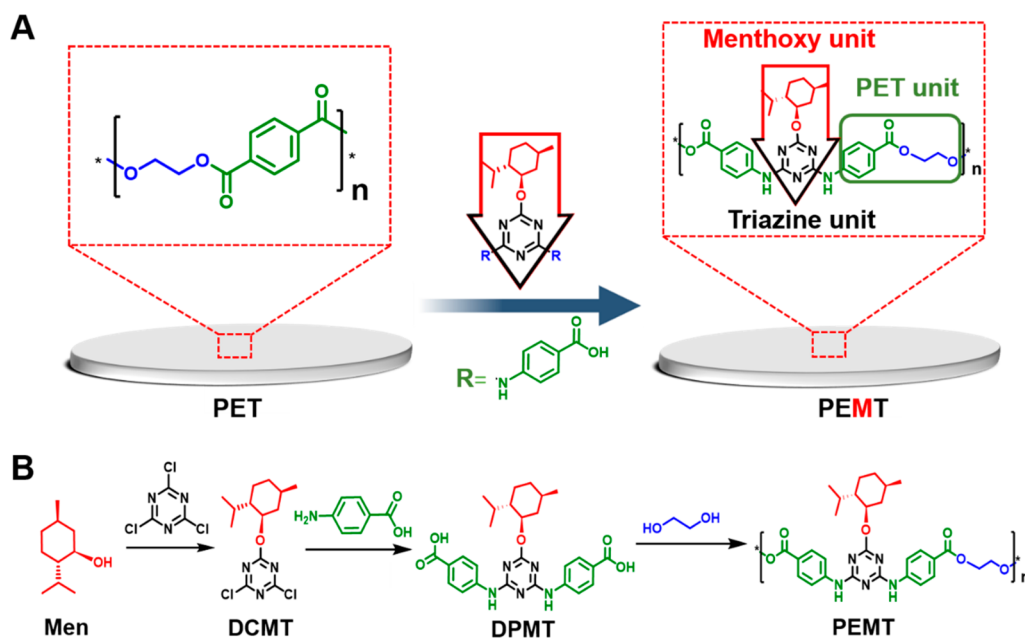
Until now, various substances with bactericidal activity, including quaternary ammonium salts (QAS),<sup>6–8</sup> metal nanoparticles<sup>9–11</sup> and *N*-halamine,<sup>12,13</sup> were introduced into PET to endow it with a strong antimicrobial performance by compounding, grafting, and other methods. For example, Wei et al. used PEG and silver nanoparticles to modify PET with a microporous structure by a composite method, and doping 1% content of silver nanoparticles gave the PET film a good antibacterial ability.<sup>11</sup> Wu et al. compounded two multi-hydroxyl *N*-halamine precursors with PET by melt blending. After the chlorination reaction, the surface of PET was endowed with strong bactericidal ability.<sup>12</sup> These studies provide ideas and references for the antimicrobial modification of PET, so it is feasible to introduce antimicrobial units to modify PET.

In recent years, a concept of stereochemistry for antimicrobial adhesion has been proposed on the basis of the “chiral taste” of microorganisms, which significantly

promotes the development in the field of antimicrobial materials.<sup>14,15</sup> This strategy limits the spread of microbial (bacteria and fungi) mainly because of the unique stereochemical structure of chiral molecules.<sup>16–18</sup> Focusing on the single-cyclic monoterpene with a stereochemical feature of borneol, a series of modified materials and polymer that control microbial adhesion have been reported.<sup>19–27</sup> For example, Wang et al. synthesized diblock copolymers from dopamine and borneol by RAFT polymerization.<sup>24</sup> The resulting polymer coatings exhibited efficient antibacterial properties. Besides, Wu et al. introduced borneol groups into polyurethanes *via* poly addition. The antimicrobial adhesion properties of the modified polyurethanes were significantly improved due to the introduction of the borneol groups.<sup>28</sup> Recently, menthol has been used as a promising candidate for stereochemical antimicrobial materials because of its unique monocyclic molecular structure. Menthol is a natural plant extract with good antibacterial and fungal abilities from a wide range of sources.<sup>29</sup> The relatively small spatial site resistance of menthol compared to the large cage-like structure of borneol

**Received:** December 6, 2021

**Accepted:** January 26, 2022

Scheme 1. Preparation Route of PEMT<sup>a</sup>

<sup>a</sup>(A) Functionalized modification of PET using menthoxytriazine. (B) Preparation roadmap of PEMT from menthol.

makes it easier to be modified to yield various menthol-derived compounds. Menthol is rarely used directly to modify PET because menthol sublimates rapidly under room temperature, a property that may cause PET to fail to achieve good antimicrobial performance.<sup>30</sup> Therefore, the insertion of menthol molecules into the polymer may be a good way to solve this problem. Triazine is a low-cost commercial available compound that readily reacts chemically with hydroxyl and amino groups because of the highly reactive chlorine atom on its ring.<sup>31–33</sup> This property of triazine makes it suitable as a carrier for polymer synthesis.<sup>34,35</sup> Li et al. successfully synthesized polyamides containing a triazine structure and exhibited good inhibition of fungal spores.<sup>36</sup> Therefore, it is promising that antimicrobial PET can be prepared by using menthoxytriazine derivatives as diacid units.

Herein, a modified strategy by inserting antiadhesive units into the backbone of PET was proposed. As shown in Scheme 1A, an antimicrobial modified PET, named PEMT, was prepared. The menthoxytriazine groups were inserted into the backbone of PET *via* polycondensation between ethylene glycol (EG) with 2-menthol-4,6-aminobenzoic-1,3,5-triazine (DPMT) (Scheme 1B for synthesis details). The *Escherichia coli* (*E. coli*, Gram-negative), *Staphylococcus aureus* (*S. aureus*, Gram-positive), and *Aspergillus niger* (*A. niger*, fungi) were employed to challenge the PEMT with an antibacterial adhesion test and the antifungal landing test, respectively. Zone of inhibition, water contact angle (CA), and BacLight live/dead fluorescent experiments were employed to further illustrate the antimicrobial mechanism. Furthermore, MTT assay was performed to demonstrate the cytotoxicity of PEMT.

## 2. EXPERIMENT

**2.1. Materials.** PET was supplied by Dongguan Hongcheng Plastic Chemical Co. (Guangdong, China). 2,4,6-Trimethyl-pyridine (99.5%), 4-aminobenzoic (PABA, 99.0%), ethylene glycol (EG, 99.0%), and *L*-menthol (Men, 99.5%) were all purchased from Shanghai Aladdin Biochemical

Technology Co., Ltd. Pyridine (Py, 99.0%), diisopropylcarbodiimide (DIC, 98.7%), and 1,3,5-triazine (99.0%) was purchased from Beijing J&K Scientific Co., Ltd. 4-(Dimethylamino)pyridinium-4-toluenesulfonate (DPTS) was prepared according to the method in the published literature.<sup>37</sup> All the solvents were of analytical grade. *Escherichia coli* (*E. coli*, ATCC 25922), *Staphylococcus aureus* (*S. aureus*, ATCC 25923), and *Aspergillus niger* (*A. niger*, CICC 41254) were obtained from the China Center of Industrial Culture Collection. Mouse fibroblast cells (L929) were obtained from Cell Resource Center, IBMS, CAMS/PUMC, Beijing, China.

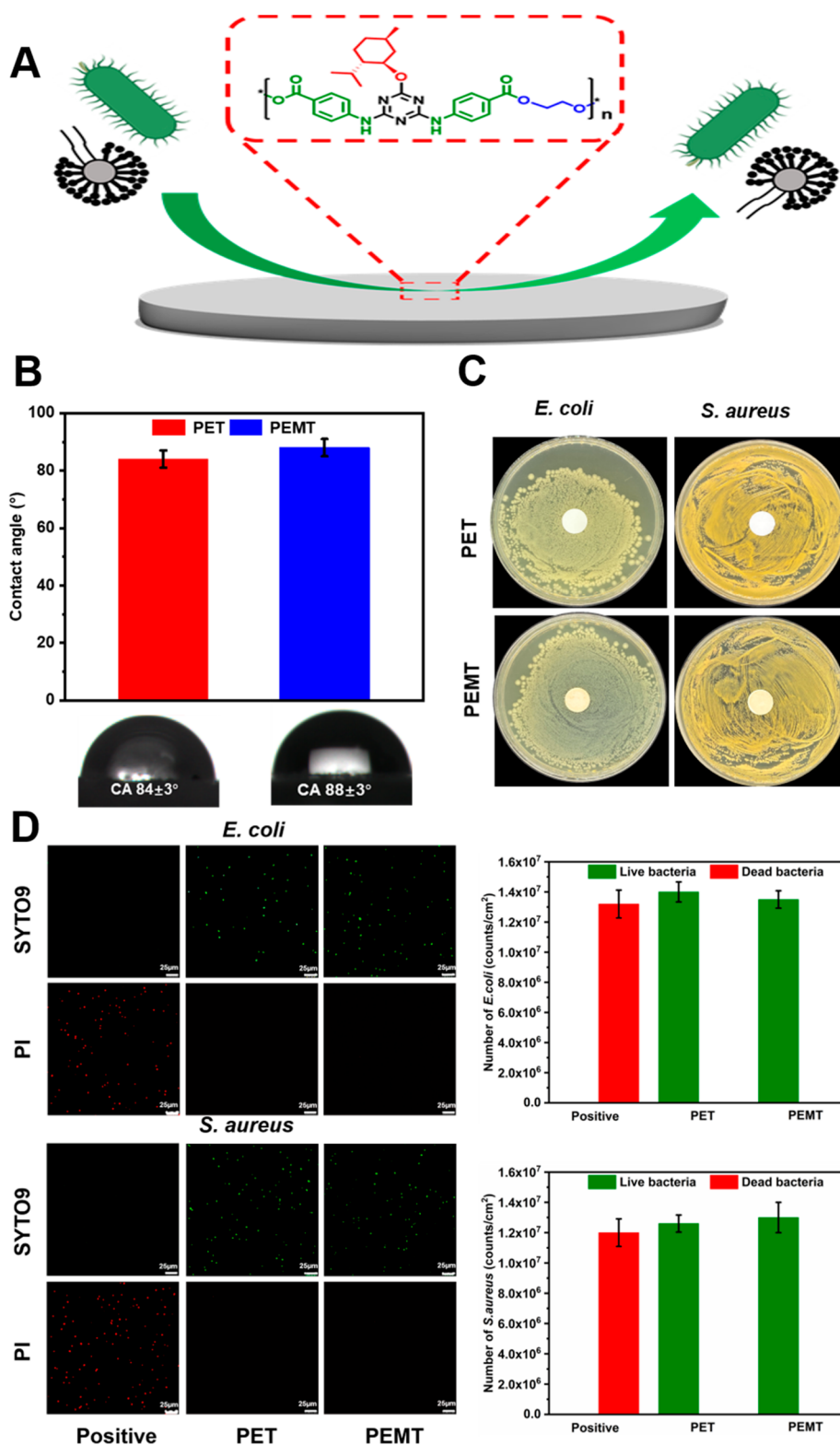
### 2.2. Preparation of 2-Menthol-1,3,5-Triazine (DCMT).

DCMT was synthesized on the basis of the literature previously reported.<sup>21</sup> *L*-Menthol (9.4 g) was completely dissolved in a solution of 20 mL of dichloromethane (DCM). 1,3,5-Triazine (5.5 g) and 4 mL of 2,4,6-trimethylpyridin were added into the mixed solution system. The reaction was stirred under an ice water bath for 12 h. The mixture was then washed four times with a large amount of deionized water (DI). The lower DCM layer was filtered, and then, the solvent was concentrated by spin evaporation. Finally, the resulting concentrated solution was purified by silica gel column chromatography (200–300 mesh, Qingdao Ocean Chemical Co.; the eluent was petroleum ether/DCM = 5:1). The final yield of the product was 80.0%.

**2.3. Preparation of 2-Menthol-4,6-PABA-1,3,5-Triazine (DPMT).** 1.8 g of DCMT, 4.1 g of PABA, and 0.2 g of pyridine were dissolved in a solution of 20 mL of *N,N*-dimethylformamide (DMF). The reaction system was maintained at 120 °C for 6 h. After the reaction temperature dropped to 25 °C, the pH of the mixed solution was adjusted to 3.0 using 10% hydrochloric acid solution, and then, the production was obtained by filtration and drying at 60 °C. The final yield was 70.0%.

**2.4. Preparation of PEMT.** The polymerization of PEMT was carried out by room temperature polymerization on the

Scheme 2. (A) Mechanisms of Microbially Antiadhesive Effect of PEMT. (B) CA of PET and PEMT. (C) ZOI Test of PET and PEMT against *E. coli* and *S. aureus*. (D) BacLight Live/Dead Fluorescent Assay of *E. coli* and *S. aureus* after 24 h of Contact with PET and PEMT, Respectively<sup>a</sup>



<sup>a</sup>The scale bar in the image is 25 μm.

basis of literature previously reported.<sup>37</sup> Under nitrogen protection, 5.0 g of DPMT, 3.3 g of EG, 0.3 g of DPTS, and 10 mL of DCM were added to the reaction flask, and the mixture was stirred until completely dissolved. Fifteen

milliliters of DIC was slowly injected into the reaction flask under an ice water bath. After 0.5 h, the temperature was raised to room temperature and the reaction continued for 96 h. Finally, the resulting viscous polymer was completely dissolved

in DCM solution and precipitated in methanol while stirring, and the above process was repeated three times to remove unreacted monomers and catalysts. The settled product was dried in a vacuum oven. The final product yield was 65.0%

**2.5. Characterization and Measurements.** Fourier transform infrared (FTIR) spectra were recorded on a Nicolet Avatar-360 spectrometer in the range 3800–500  $\text{cm}^{-1}$ .  $^1\text{H}$  NMR spectra were determined by a Bruker AV-500 spectrometer at 400 MHz using DMSO as deuterated solvents. The molecular mass of polymers was tested by gel permeation chromatography (GPC) with an Agilent instrument (Model 1100). Material surface wettability was measured by a CA-XPI50 measuring instrument.

**2.6. Bacterial Antiadhesion Assays.** According to previous reports, a visual antibacterial spreading test was first performed.<sup>38</sup> PEMT was pressed into a regular circular sheet with a diameter of 13 mm and a thickness of 0.75 mm. A “sandwich structure” was utilized to enable the visualization of antibacterial adhesion evaluation (Scheme 2A). The bottom layer was TSA medium (thickness = 5 mm, diameter = 90 mm), the middle layer was round material (thickness = 0.75 mm, diameter = 13 mm), and the top layer was TSA medium (thickness = 5 mm, diameter = 4 mm). A preprepared 2  $\mu\text{L}$  suspension of *E. coli* or *S. aureus* at a concentration of  $10^6$  CFU  $\text{mL}^{-1}$  was dropped on the topmost “isolated TSA island”, and the plates were then placed in a bacterial incubator at 37 °C. Bacterial growth was recorded with a digital camera every 24 h. Pure PET was used as a control.

In addition, a quantitative test based on previous reports was also used to assess the antibacterial adhesion properties of PEMT.<sup>28</sup> Both sides of PEMT were irradiated with UV for 15 min. Next, the PEMT sheets were completely submerged in 1 mL of bacterial suspension at a concentration of  $10^6$  CFU  $\text{mL}^{-1}$ . After 24 h, PEMT was gently rinsed three times with DI water to avoid the influence of bacteria floating on the surface of the material on the results. Then, PEMT was submerged in 2 mL of PBS solution and ultrasonicated for 10 min with a power of 50 W to ensure that the bacteria adhering to the surface of PEMT were dispersed in the solution. Then, 100  $\mu\text{L}$  of the diluted bacterial dispersion was taken to be evenly coated on TSA medium and subsequently incubated in a bacterial incubator at 37 °C for 24 h. Bacterial growth was recorded using a digital camera. Colony-forming units (CFUs) were calculated, and the following equation was used to calculate the rate of antibacterial adhesion of the material:

$$\text{antibacterial adhesion rate (\%)} = (A - B)/A \times 100$$

where *A* and *B* are the CFUs of pure PET and PEMT, respectively.

In addition, PEMT was subjected to five “contact-sterilization-recontact” cycles to test its reproducible antimicrobial adhesion performance. Pure PET was used as a control.

**2.7. Fungal Repelling Assays.** The antifungal properties of PEMT were studied by “antifungal landing test” according to previously reported method.<sup>39</sup> PEMT was pressed into a regular circular sheet with a diameter of 13 mm and a thickness of 0.75 mm. A preprepared suspension of 2  $\mu\text{L}$  of *A. niger* suspension at a concentration of  $10^6$  CFU  $\text{mL}^{-1}$  was added to the center of the wort medium. Next, PEMT was placed approximately 15 mm from the center. Plates were placed in a fungal incubator at 30 °C. The growth of *A. niger* in the plates was recorded every 24 h using a digital camera. The antifungal

properties of PEMT were quantified by measuring the area of fungal colonization using an ImageJ software package. Pure PET was used as a control.

**2.8. Zone of Inhibition (ZOI) Experiment.** A ZOI experiment was used to test whether the material is sterilized by releasing small molecule. Bacterial suspension (100  $\mu\text{L}$ ) with a concentration of  $10^6$  CFU  $\text{mL}^{-1}$  was dropped onto the TSA medium; then, the bacterial suspension was spread evenly with a spreader. PEMT was placed on the center of the medium, and the plates were incubated at a constant temperature of 37 °C for 24 h. Whether there was a ZOI was recorded by the digital camera.

**2.9. BacLight Live/Dead Fluorescent Assay.** The BacLight live/dead fluorescent staining method was chosen to investigate whether PEMT caused a reduction in colony count by contact sterilization. Twenty microliters of suspension of *E. coli* or *S. aureus* with a concentration of  $10^9$  CFU  $\text{mL}^{-1}$  was dropped on the surface of PEMT, and the PE film was gently placed over the material to ensure adequate contact between the suspension and the material. After the material was kept at 4 °C for 24 h, PEMT (including PE film and bacterial suspension) was submerged in 1 mL of PBS solution and the solution was sonicated for 10 min with a power of 50 W to ensure that all bacteria were dispersed in the solution. One microliter of 3.3 mM SYTO9 and 1  $\mu\text{L}$  of 30.0 mM PI were added to the above bacterial suspension. The mixture was held in the dark in an incubator at 37 °C for 20 min and then washed with saline and centrifuged. One hundred microliters of the stained bacterial suspension was dropped onto a confocal dish. The staining was then observed with a confocal microscope. A commercial AgNPs/PET was selected as a positive control for fluorescent staining. Bacteria on the different samples were quantified by ImageJ (version 1.8.0).

**2.10. Cytotoxicity Assays.** MTT cytocompatibility assay was used to verify whether PEMT was cytotoxic. It was first thoroughly sterilized by UV irradiation of 0.2 g of PET or PEMT for 30 min. Afterward, the material was soaked in 2 mL of 1640 medium for 24 h to obtain the infusion solution. Then, 10% FBS, 100 units  $\text{mL}^{-1}$  penicillin, and 100  $\mu\text{g mL}^{-1}$  streptomycin were added to the extract to configure the complete cell culture medium. L929 mouse fibroblasts were inoculated in the above medium and the culture dishes were placed in a cell culture incubator at 37 °C for 48 h. Finally, the cells were stained with a MTT assay kit, and cell viability was determined using a UV spectrophotometer. The relative growth rate (RGR) of the cells was calculated using the following equation:

$$\text{RGR (\%)} = \text{Abs}_{490\text{sample}}/\text{Abs}_{490\text{control}} \times 100$$

where  $\text{Abs}_{490\text{ sample}}$  and  $\text{Abs}_{490\text{ control}}$  represent the absorbance at 490 nm of the sample and control groups, respectively.

## 3. RESULTS AND DISCUSSION

**3.1. Preparation and Characterization of PEMT.** PEMT was prepared by a three-step process (Scheme 1B). To produce a polymerizable diacid monomer, DCMT was first synthesized by the substitution reaction occurring between 1,3,5-triazine and *L*-menthol. Then, polymerizable diacid monomer (DPMT) was synthesized by the nucleophilic substitution of DCMT and PABA. Finally, polymer was synthesized by the room temperature polycondensation

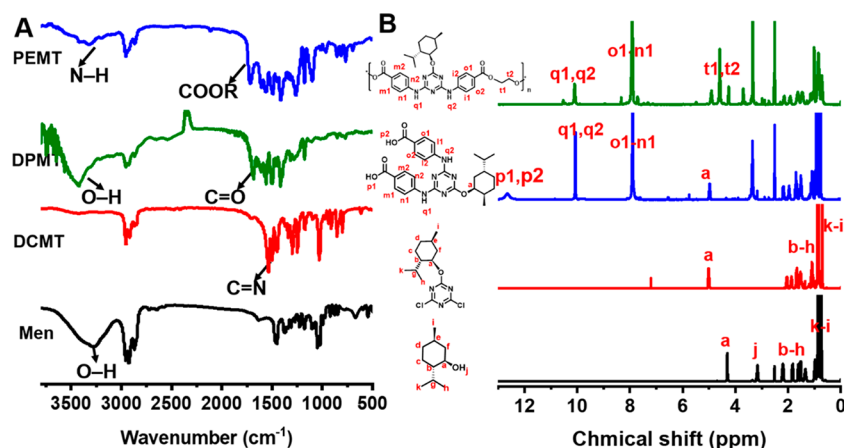


Figure 1. (A) FTIR spectra of Men, DCMT, DPMT, and PEMT. (B) <sup>1</sup>H NMR spectra of Men, DCMT, DPMT, and PEMT.

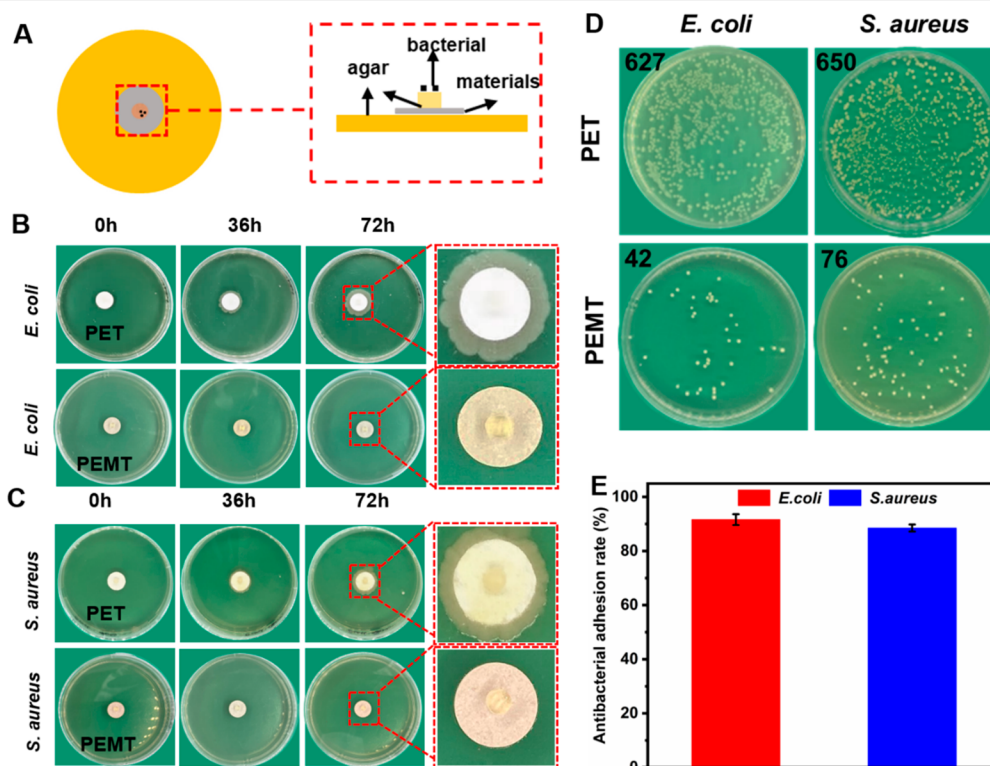


Figure 2. (A) Schematic diagram of antibacterial spreading test. (B) Photographs of agar plates of *E. coli* in the PET and PEMT groups within 72 h. (C) Photographs of agar plates of *S. aureus* in the PET and PEMT groups within 72 h. (D) Result of plate count of PET and PEMT against *E. coli* and *S. aureus*. (E) Antibacterial adhesion rate of PET and PEMT against *E. coli* and *S. aureus*.

strategy. FTIR were first performed in order to determine the composition of the PEMT polymer.

In the FTIR spectra, the broad adsorption band at 3300 cm<sup>-1</sup> corresponds to the stretching vibration of the hydroxyl group of menthol (Figure 1A, black). After the one-substitution reaction with triazine, the hydroxyl peak at 3300 cm<sup>-1</sup> disappeared and a new absorption peak appeared centered at 1500 cm<sup>-1</sup>, which represented the stretching vibrations of vibration of the triazine group on DCMT. When the other two chlorine atoms on the triazine were replaced by PABA, the broad peak at 3330 cm<sup>-1</sup> represents the O–H and N–H stretching absorption (Figure 1A, blue). In addition, the new peaks at 1678 and 1310 cm<sup>-1</sup> indicated the presence of the carboxyl ester group. The new absorption peak at 1510

cm<sup>-1</sup> was assigned to the hydroxyl group of carboxylic acid. In the FTIR spectrum of PEMT (Figure 1A, green), the absorption peaks at 1678 and 1510 cm<sup>-1</sup> representing the ester and hydroxyl groups of the carboxylic acid disappeared, respectively. A new absorption peak at 1718 cm<sup>-1</sup> can be assigned to the ester functional group of the polyester.

In addition, <sup>1</sup>H NMR was used in order to further identify the chemical structures of monomers and polymer. In the <sup>1</sup>H NMR spectra of DCMT (Figure 1B, red), compared with those of Men (Figure 1A, black), the resonance signal of the hydroxyl group at 4.20 ppm completely disappeared, indicating that the hydroxyl group on menthol was successfully substituted. In terms of DPMT (Figure 1B, blue), the newly appearing signal peaks at 7.98, 10.00, and 12.30 ppm

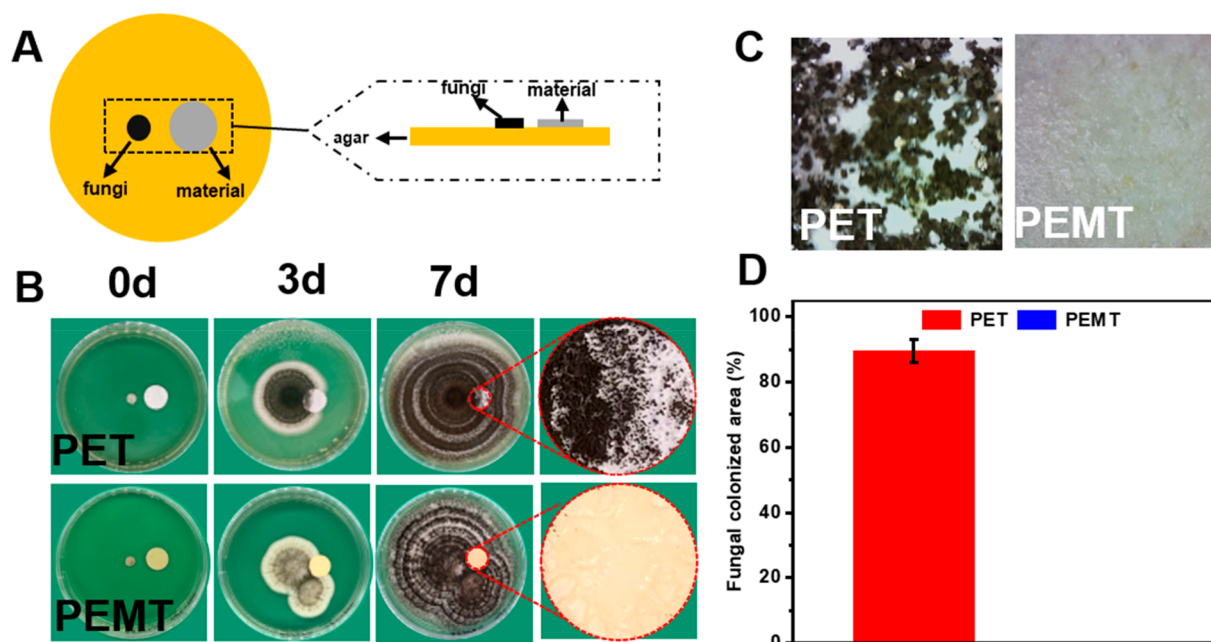


**Figure 3.** (A) Schematic illustration of “antifungal landing test”. (B) Photographs of the growth of *A. niger* in the PET and PEMT groups within 72 h. (C) Micrographs of PET and PEMT surfaces at day 7. (D) Quantification of fungal colonization areas on PET and PEMT surfaces.

represented resonances of protons of aromatic, imino, and carboxylic acid groups, respectively. In the  $^1\text{H}$  NMR spectrum of PEMT, the signal peak at 7.98 ppm represented the proton of methylene (Figure 1B, green). The signal peak representing the carboxylic acid proton disappeared at 12.30 ppm, indicating that esterified dehydration occurred between DPMT and EG. Polymer had a high molecular weight ( $M_w = 1.12 \times 10^4 \text{ g mol}^{-1}$ ) and a narrow distribution of relative molecular masses ( $\text{PDI} = 1.02$ ) (Table S1). The content of the menthoxy block in the PEMT was 28.16%.

**3.2. Bacterial Antiadhesion Assays.** The antibacterial adhesion activity of PEMT was tested by an antibacterial spreading test first (Figure 2A). It could be found that the growth of *E. coli* broke the limit of PET, and the bacterial ring could be observed clearly after 36 h, indicating that PET did not have any inhibiting ability on the growth and spread of *E. coli*. On the contrary, the *E. coli* in PEMT group did not break the limit until 72 h, leading to the appearance of bacterial ring (Figure 2B). Similar to the results of *E. coli*, *S. aureus* broke the restriction of PET after 36 h, while PEMT was not broken. The inhibition of *S. aureus* growth by PEMT was maintained for 72 h (Figure 2C). Thus, PEMT showed better capability of inhibiting the spread of *E. coli* and *S. aureus*, compared to the PET. The antibacterial adhesion properties of PEMT were also studied quantitatively by a live bacteria count. The results of live bacterial counts showed that the colony counts of PET were much larger than those of PEMT for both *E. coli* and *S. aureus* (Figure 2D), which indicated that PEMT possessed better adherence against bacteria, compared to PET. In addition, the antibacterial adhesion rate of PEMT to *E. coli* was 93.3%, while that to *S. aureus* was 88.3% (Figure 2E). The antiadhesive effect of PEMT against *E. coli* was better than that against *S. aureus*, which may be due to the differences in antiadhesive performance of chiral terpene molecules like menthol to bacteria with different structures.<sup>28</sup> The results of repeat antiadhesive test indicated that PEMT was reusable, since no significant decrease of the antibacterial adhesion rate

was found after five “contact-sterilization-recontact” cycles (Figure S5).

**3.3. Fungal Repelling Assays.** The antifungal landing test was used to evaluate the antifungal properties of PEMT (Figure 3A). After 3 d of incubation, the growth of *A. niger* on the surface of PET and PEMT showed a difference visible to the naked eye. When *A. niger* grew to contact with PET, it chose to continue spreading to the PET surface. In contrast, *A. niger* chose to bypass PEMT and continue growing on the medium. This difference was significantly amplified after 7 d (Figure 3B). PET was almost completely covered by *A. niger* spores, while there was still no growth of *A. niger* on the surface of PEMT. The micrographs of PET and PEMT showed that a high density of fungi covered the surface of PET, while the surface of PEMT was still clean without any *A. niger* (Figure 3C). The fungal coverage of the PET surface reached more than 90.0% after 7 d, while the PEMT surface remained 0% (Figure 3D). Thus, compared with PET, PEMT had excellent capability to inhibit the growth of *A. niger*.

**3.4. Analysis of Antiadhesive Mechanisms.** The emergence of superbugs proves that a single-minded approach to sterilization is not ideal.<sup>40</sup> Menthol is a monocyclic terpene molecule that fits into a stereochemical antimicrobial strategy.<sup>27</sup> The PEMT prepared by this strategy showed antimicrobial properties, due to the unique stereochemical structure of the menthoxy group. The advantage of this strategy over the reported antimicrobial strategies is that it can effectively control the adhesion of external harmful microorganisms and is expected to avoid the development of drug resistance.<sup>41</sup> Bacteria and fungi are living organisms at the cellular level and are expected to be able to distinguish between microorganisms with different stereochemical surfaces on which they have different adhesion and growth behaviors. Thus, due to the recognition function of microorganism to the chiral structure of menthoxy, when the microorganism was close to the material, it would choose to avoid the material and continue to spread (Scheme 2A).<sup>16,41,42</sup> It is known that the

wettability of material affects its antimicrobial properties. Thus, the CA of PET and PEMT were tested. As showed in Scheme 2B, the CA of the two materials were  $84.0 \pm 3.0^\circ$  and  $88.0 \pm 3.0^\circ$ , indicating that the difference in wettability between PEMT and PET was negligible. It demonstrated that the antimicrobial properties of PEMT were not related to the wettability of the material. At the same time, a ZOI test was used to confirm the presence of releasing germicide in PEMT (Scheme 2C). As we can see, there was no inhibition zone against *E. coli* and *S. aureus*. Thus, PEMT was a nonleaching material. Furthermore, fluorescent staining experiments were performed to investigate whether PEMT achieves its antimicrobial effect by killing bacteria (Scheme 2D). After 24 h of contact with the bacterial suspension, the positive control group could only be observed with red fluorescence of *E. coli* or *S. aureus*, indicating that the bacteria were all killed. On the contrary, only green fluorescence was observed on PET and PEMT samples, which indicated that the samples did not have a bacteria-killing property. In addition, the quantitative data for both strains also showed no significant difference in the number of live bacteria between PET and PEMT. It suggested that PEMT did not achieve its antiadhesion effect by directly killing bacteria. All the above evidence suggested that the antiadhesive properties of PEMT were attributed to the stereochemical structure of the menthol unit.

**3.5. MTT Assay.** MTT assay was conducted to evaluate the cytotoxicity of the material (Figure 4). The relative growth

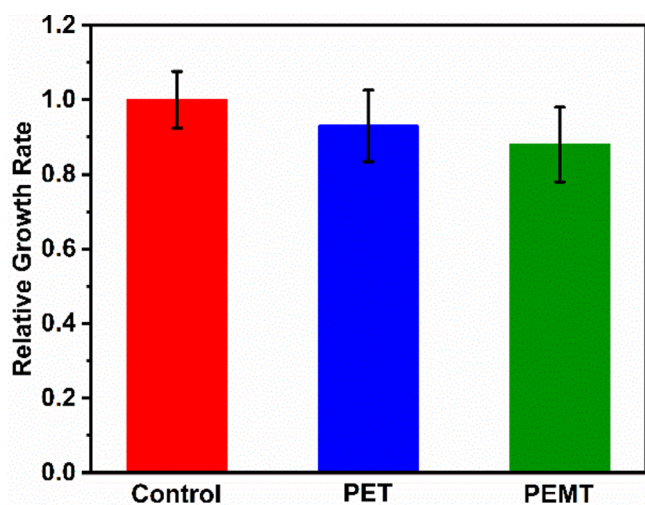


Figure 4. MTT results for PET and PEMT.

rates (RGRs) of L929 cells for PET and PEMT were both more than 80.0% (Figure 4). According to the internationally recognized toxicity rating standard, the cell toxicity of PET and PEMT was grade 1 (Table S2). Therefore, PEMT was a noncytotoxic material.

#### 4. CONCLUSION

In summary, PEMT, a PET containing menthoxytriazine, was prepared by typical polycondensation between DPMT and EG for the inhibition of microbial adhesion. PEMT possessed good antimicrobial adhesion properties with antibacterial adhesion rates of 93.3% and 88.3% against *E. coli* and *S. aureus*, respectively, and effective inhibition of *A. niger* for 7 d. The antimicrobial mechanism of PEMT was attributed to stereochemistry strategy rather than bactericide or wettability.

In addition, PEMT was a noncytotoxic polymer. These results indicated that PEMT was a promising candidate for antimicrobial PET. Moreover, the modification strategy of inserting antimicrobial triazine-derivatives into the PET backbone is feasible and provides a versatile platform for designing antimicrobial PET.

#### ■ ASSOCIATED CONTENT

##### Supporting Information

The Supporting Information is available free of charge at <https://pubs.acs.org/doi/10.1021/acsapm.1c01775>.

Figures of  $^1\text{H}$  NMR spectra, GPC results, and antibacterial adhesion rate of PEMT and tables of GPC results for the PEMT and MTT results for the PEMT and PET (PDF)

#### ■ AUTHOR INFORMATION

##### Corresponding Authors

**Guofeng Li** – Beijing Laboratory of Biomedical Materials, College of Life Science and Technology, Beijing University of Chemical Technology, Beijing 100029, P. R. China; Email: [chase.lg@163.com](mailto:chase.lg@163.com)

**Xing Wang** – Beijing Laboratory of Biomedical Materials, College of Life Science and Technology, Beijing University of Chemical Technology, Beijing 100029, P. R. China; [orcid.org/0000-0002-9990-1479](https://orcid.org/0000-0002-9990-1479); Email: [wangxing@mail.buct.edu.cn](mailto:wangxing@mail.buct.edu.cn)

##### Authors

**Jiyu Li** – Beijing Laboratory of Biomedical Materials, College of Life Science and Technology, Beijing University of Chemical Technology, Beijing 100029, P. R. China

**Pengfei Zhang** – Beijing Laboratory of Biomedical Materials, College of Life Science and Technology, Beijing University of Chemical Technology, Beijing 100029, P. R. China

**Mei Yang** – Beijing Laboratory of Biomedical Materials, College of Life Science and Technology, Beijing University of Chemical Technology, Beijing 100029, P. R. China

**Zixu Xie** – Beijing Laboratory of Biomedical Materials, College of Life Science and Technology, Beijing University of Chemical Technology, Beijing 100029, P. R. China

Complete contact information is available at: <https://pubs.acs.org/10.1021/acsapm.1c01775>

##### Author Contributions

#J.L. and P.Z. contributed equally to this work.

##### Notes

The authors declare no competing financial interest.

#### ■ ACKNOWLEDGMENTS

The authors would like to thank the National Natural Science Foundation of China (21574008) and the Fundamental Research Funds for the Central Universities of China (BHYC1705B) for their financial support.

#### ■ REFERENCES

- (1) Roger, P.; Renaudie, L.; Le Narvor, C.; Lepoittevin, B.; Bech, L.; Brogly, M. Surface Characterizations of Poly(Ethylene Terephthalate) Film Modified by a Carbohydrate-Bearing Photoreactive Azide Group. *Eur. Polym. J.* **2010**, *46*, 1594–1603.
- (2) Ding, L.; Liu, L.; Chen, Y. F.; Du, Y.; Guan, S. J.; Bai, Y.; Huang, Y. Modification of Poly(Ethylene Terephthalate) by Copolymeriza-

tion of Plant-Derived A-Truxillic Acid with Excellent Ultraviolet Shielding and Mechanical Properties. *Chem. Eng. J.* **2019**, *374*, 1317–1325.

(3) Ping, X.; Wang, M.; Xuewu, G. Surface Modification of Poly(Ethylene Terephthalate) (PET) Film by Gamma-Ray Induced Grafting of Poly(Acrylic Acid) and Its Application in Antibacterial Hybrid Film. *Radiat. Phys. Chem.* **2011**, *80*, 567–572.

(4) Çaykara, T.; Sande, M. G.; Azoia, N.; Rodrigues, L. R.; Silva, C. J. Exploring the Potential of Polyethylene Terephthalate in the Design of Antibacterial Surfaces. *Med. Microbiol. Immunol.* **2020**, *209*, 363–372.

(5) Bedel, S.; Lepoittevin, B.; Costa, L.; Leroy, O.; Dragoe, D.; Bruzard, J.; Herry, J.-M.; Guilbaud, M.; Bellon-Fontaine, M.-N.; Roger, P. Antibacterial Poly(Ethylene Terephthalate) Surfaces Obtained from Thymyl Methacrylate Polymerization. *J. Polym. Sci. Part A Polym. Chem.* **2015**, *53*, 1975–1985.

(6) Zhang, S.; Li, R.; Huang, D.; Ren, X.; Huang, T. S. Antibacterial Modification of PET with Quaternary Ammonium Salt and Silver Particles via Electron-Beam Irradiation. *Mater. Sci. Eng., C* **2018**, *85*, 123–129.

(7) Min, T.; Zhu, Z.; Sun, X.; Yuan, Z.; Zha, J.; Wen, Y. Highly Efficient Antifogging and Antibacterial Food Packaging Film Fabricated by Novel Quaternary Ammonium Chitosan Composite. *Food Chem.* **2020**, *308*, 125682.

(8) Çitak, E.; Testici, H.; Gürsoy, M.; Sevgili, E.; Dağ, H. T.; Öztürk, B.; Karaman, M. Vapor Deposition of Quaternary Ammonium Methacrylate Polymers with High Antimicrobial Activity: Synthetic Route, Toxicity Assessment, and Durability Analysis. *J. Vac. Sci. Technol. A* **2020**, *38*, 043203.

(9) Naeem, M.; Felipe, M. B. M. C.; de Medeiros, S. R. B.; Costa, T. H. C.; Libório, M. S.; Alves, C.; Nascimento, R. M.; Nascimento, I. O.; Sousa, R. R. M.; Feitor, M. C. Novel Antibacterial Silver Coating on PET Fabric Assisted with Hollow-Cathode Glow Discharge. *Polym. Adv. Technol.* **2020**, *31*, 2896–2905.

(10) Bashiri Rezaie, A.; Montazer, M.; Mahmoudi Rad, M. Low Toxic Antibacterial Application with Hydrophobic Properties on Polyester through Facile and Clean Fabrication of Nano Copper with Fatty Acid. *Mater. Sci. Eng., C* **2019**, *97*, 177–187.

(11) Wei, S.; Qian, K.; Pan, M.; Li, Y.; Raidron, C.; Wang, Y. Preparation and Properties of Micropore Structure Polyethylene Terephthalate Films Modified with PEG and Nano-Ag Particles and Its Antibacterial Characteristics. *Polym. Plast. Technol. Eng.* **2015**, *54*, 565–572.

(12) Wu, K.; Li, J.; Chen, X.; Yao, J.; Shao, Z. Synthesis of Novel Multi-Hydroxyl N-Halamine Precursors Based on Barbituric Acid and Their Applications in Antibacterial Poly(Ethylene Terephthalate) (PET) Materials. *J. Mater. Chem. B* **2020**, *8*, 8695.

(13) Kim, S. S.; Kim, J.; Huang, T. S.; Whang, H. S.; Lee, J. Antimicrobial Polyethylene Terephthalate (PET) Treated with an Aromatic N-Halamine Precursor, m-Aramid. *J. Appl. Polym. Sci.* **2009**, *114*, 3835–3840.

(14) Luo, L.; Li, G.; Luan, D.; Yuan, Q.; Wei, Y.; Wang, X. Antibacterial Adhesion of Borneol-Based Polymer via Surface Chiral Stereochemistry. *ACS Appl. Mater. Interfaces* **2014**, *6*, 19371–19377.

(15) Zhang, P.; Yang, M.; Li, J.; Xie, Z.; Li, G.; Wang, X. Menthoxytriazine Modified Poly(Ethylene Terephthalate) for Constructing Anti-Adhesion Surface. *Colloid Interface Sci. Commun.* **2022**, *46*, 100567.

(16) Li, G.; Zhao, H.; Hong, J.; Quan, K.; Yuan, Q.; Wang, X. Antifungal Graphene Oxide-Borneol Composite. *Colloids Surf., B* **2017**, *160*, 220–227.

(17) Xu, J.; Bai, Y.; Wan, M.; Liu, Y.; Tao, L.; Wang, X. Antifungal Paper Based on a Polyborneolacrylate Coating. *Polymers*. **2018**, *10*, 448.

(18) Chen, C.; Xie, Z.; Zhang, P.; Liu, Y.; Wang, X. Cooperative Enhancement of Fungal Repelling Performance by Surface Photografting of Stereochemical Bi-Molecules. *Colloids Interface Sci. Commun.* **2021**, *40*, 100336.

(19) Yang, L.; Zhan, C.; Huang, X.; Hong, L.; Fang, L.; Wang, W.; Su, J. Durable Antibacterial Cotton Fabrics Based on Natural Borneol-Derived Anti-MRSA Agents. *Adv. Healthc. Mater.* **2020**, *9*, 2000186.

(20) Hu, J.; Sun, B.; Zhang, H.; Lu, A.; Zhang, H.; Zhang, H. Terpolymer Resin Containing Bioinspired Borneol and Controlled Release of Camphor: Synthesis and Antifouling Coating Application. *Sci. Rep.* **2020**, *10*, 10375.

(21) Cheng, Q.; Asha, A. B.; Liu, Y.; Peng, Y. Y.; Diaz-Dussan, D.; Shi, Z.; Cui, Z.; Narain, R. Antifouling and Antibacterial Polymer-Coated Surfaces Based on the Combined Effect of Zwitterions and the Natural Borneol. *ACS Appl. Mater. Interfaces* **2021**, *13* (7), 9006–9014.

(22) Xin, Y.; Zhao, H.; Xu, J.; Xie, Z.; Li, G.; Gan, Z.; Wang, X. Borneol-Modified Chitosan: Antimicrobial Adhesion Properties and Application in Skin Flora Protection. *Carbohydr. Polym.* **2020**, *228*, 115378.

(23) Song, F.; Zhang, L.; Chen, R.; Liu, Q.; Liu, J.; Yu, J.; Liu, P.; Duan, J.; Wang, J. Bioinspired Durable Antibacterial and Antifouling Coatings Based on Borneol Fluorinated Polymers: Demonstrating Direct Evidence of Antiadhesion. *ACS Appl. Mater. Interfaces* **2021**, *13*, 33417–33426.

(24) Wang, X.; Jing, S.; Liu, Y.; Liu, S.; Tan, Y. Diblock Copolymer Containing Bioinspired Borneol and Dopamine Moieties: Synthesis and Antibacterial Coating Applications. *Polymer*. **2017**, *116*, 314–323.

(25) Chen, X.; Nie, Q.; Shao, Y.; Wang, Z.; Cai, Z. TiO<sub>2</sub> Nanoparticles Functionalized Borneol-Based Polymer Films with Enhanced Photocatalytic and Antibacterial Performances. *Environ. Technol. Innov.* **2021**, *21*, 101304.

(26) Yang, L.; Zhan, C.; Huang, X.; Hong, L.; Fang, L.; Wang, W.; Su, J. Durable Antibacterial Cotton Fabrics Based on Natural Borneol-Derived Anti-MRSA Agents. *Adv. Healthc. Mater.* **2020**, *9*, 2000186.

(27) Xu, J.; Xie, Z.; Du, F.; Wang, X. One-Step Anti-Superbug Finishing of Cotton Textiles with Dopamine-Menthol. *J. Mater. Sci. Technol.* **2021**, *69*, 79–88.

(28) Wu, J.; Wang, C.; Mu, C.; Lin, W. A Waterborne Polyurethane Coating Functionalized by Isobornyl with Enhanced Antibacterial Adhesion and Hydrophobic Property. *Eur. Polym. J.* **2018**, *108*, 498–506.

(29) Kamatou, G. P. P.; Vermaak, I.; Viljoen, A. M.; Lawrence, B. M. Menthol: A Simple Monoterpene with Remarkable Biological Properties. *Phytochemistry* **2013**, *96*, 15–25.

(30) Wu, X.; Li, P.; Cong, L.; Yu, H.; Zhang, D.; Yue, Y.; Xu, H.; Xu, K.; Zheng, X.; Wang, X. Electrospun Poly(Vinyl Alcohol) Nanofiber Films Containing Menthol/ $\beta$ -Cyclodextrin Inclusion Complexes for Smoke Filtration and Flavor Retention. *Colloids Surf., A* **2020**, *605*, 125378.

(31) Nasrollahzadeh, M.; Motahharifar, N.; Nezafat, Z.; Shokouhimehr, M. Copper(II) Complex Anchored on Magnetic Chitosan Functionalized Trichlorotriazine: An Efficient Heterogeneous Catalyst for the Synthesis of Tetrazole Derivatives. *Colloid Interface Sci. Commun.* **2021**, *44*, 100471.

(32) Wu, J.; Zhang, C.; Xu, S.; Pang, X.; Cai, G.; Wang, J. Preparation of Zwitterionic Polymer-Functionalized Cotton Fabrics and the Performance of Anti-Biofouling and Long-Term Biofilm Resistance. *Colloid Interface Sci. Commun.* **2018**, *24*, 98–104.

(33) Saito, K.; Nishimura, N.; Sasaki, S.; Oishi, Y.; Shibasaki, Y. Synthesis of Polyguanamines from 2-N,N-Dibutylamino-4,6-Dichloro-1,3,5-Triazine with Aromatic Diamines. *React. Funct. Polym.* **2013**, *73*, 756–763.

(34) Asundaria, S. T.; Patel, P. R.; Patel, K. C. Novel Copolyesters Based on S-Triazine Derivatives. *Int. J. Polym. Mater. Polym. Biomater.* **2009**, *58*, 692–705.

(35) Pathan, S.; Ahmad, S. S-Triazine Ring-Modified Waterborne Alkyd: Synthesis, Characterization, Antibacterial, and Electrochemical Corrosion Studies. *ACS Sustain. Chem. Eng.* **2013**, *1*, 1246–1257.

(36) Li, X.; Xie, Z.; Li, G.; Tao, L.; Wei, Y.; Wang, X. Antifungal Polymer Containing Menthoxy Triazine. *ACS Appl. Polym. Mater.* **2021**, *3* (8), 3702–3707.

(37) Chamsaz, E. A.; Sun, S.; Maddipatla, M. V. S. N.; Joy, A. Photoresponsive Polyesters by Incorporation of Alkoxyphenacyl or Coumarin Chromophores along the Backbone. *Photochem. Photobiol. Sci.* **2014**, *13*, 412–421.

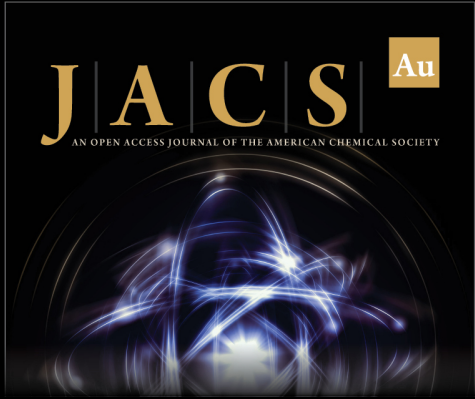
(38) Sun, X.; Qian, Z.; Luo, L.; Yuan, Q.; Guo, X.; Tao, L.; Wei, Y.; Wang, X. Antibacterial Adhesion of Poly(Methyl Methacrylate) Modified by Borneol Acrylate. *ACS Appl. Mater. Interfaces* **2016**, *8*, 28522–28528.

(39) Zhang, P.; Li, J.; Yang, M.; Huang, L.; Bu, F.; Xie, Z.; Li, G.; Wang, X. Inserting Menthoxytriazine into Poly(Ethylene Terephthalate) for Inhibiting Microbial Adhesion. *ACS Biomater. Sci. Eng.*, in press, **2021**.

(40) Gray, D. A.; Wenzel, M. Multitarget Approaches against Multiresistant Superbugs. *ACS Infect. Dis.* **2020**, *6*, 1346–1365.

(41) Xu, J.; Zhao, H.; Xie, Z.; Ruppel, S.; Zhou, X.; Chen, S.; Liang, J. F.; Wang, X. Stereochemical Strategy Advances Microbially Antiadhesive Cotton Textile in Safeguarding Skin Flora. *Adv. Healthc. Mater.* **2019**, *8*, 1900232.

(42) Hook, A. L.; Chang, C. Y.; Yang, J.; Lockett, J.; Cockayne, A.; Atkinson, S.; Mei, Y.; Bayston, R.; Irvine, D. J.; Langer, R.; Anderson, D. G.; Williams, P.; Davies, M. C.; Alexander, M. R. Combinatorial Discovery of Polymers Resistant to Bacterial Attachment. *Nat. Biotechnol.* **2012**, *30*, 868–875.



**JACS Au**  
AN OPEN ACCESS JOURNAL OF THE AMERICAN CHEMICAL SOCIETY

 Editor-in-Chief  
**Prof. Christopher W. Jones**  
Georgia Institute of Technology, USA

**Open for Submissions** 

pubs.acs.org/jacsau  ACS Publications  
Most Trusted. Most Cited. Most Read.